Human Vital Sign Determination using Tactile Sensing and Fuzzy Triage System

Emmett Kerr[a], TM McGinnity[a,b], Sonya Coleman[a], Andrea Shepherd[c]

[a]*Intelligent Systems Research Centre, University of Ulster, Magee Campus, Northern Ireland.*
[b]*Department of Computer Science, School of Science and Technology, Nottingham Trent University, UK.*
[c]*School of Nursing, University of Ulster, Magee Campus, Northern Ireland.*

Abstract

The ability to quickly and accurately triage a person's medical condition in an emergency situation or other critical scenarios could mean the difference between life and death. Endowing a robotic system with vision and tactile capabilities, similar to those of medical professionals, and thus enabling robots to assess a patient's status in an emergency is a highly sought after characteristic in healthcare robotics. This paper presents a novel fuzzy triage system exploiting visual and tactile sensing, to equip a robot with the skills to accurately determine key vital signs in humans. There are three key signs of human health: respiratory rate, pulse rate (Beats Per Minute (BPM)) and capillary refill time. Using ground truth from a medical professional, the fuzzy triage system is trained and validated initially with informed synthetic data and then further evaluated using vital signs data collected from subjects in a pilot study. Results from this pilot study indicate that the fuzzy triage system is capable of classifying a patient's health using the the novel approaches for collecting BPM, Respiratory Rate (RR) and Capillary Refill Time (CRT) which replicate, to some extent, the approaches used by medical professionals for measuring vital signs. Furthermore, the intelligent system proved capable of determining whether a pulse was regular or arrhythmic, whether respiratory

Email addresses: ep.kerr@ulster.ac.uk (Emmett Kerr), martin.mcginnity@ntu.ac.uk (TM McGinnity), tm.mcginnity@ulster.ac.uk (TM McGinnity), sa.coleman@ulster.ac.uk (Sonya Coleman), a.shepherd@ulster.ac.uk (Andrea Shepherd)

rate was regular or irregular, and determining the subject's capillary refill time. Such results imply that this system could ultimately be used, for example, in a home assistance robot for elderly or disabled persons, or as a first responder robot. Ultimately the aim would be that these methods could be utilised by robotic systems in emergency scenarios or disaster zones.

Keywords: Fuzzy Systems, Automated Triage, Signal Processing, Tactile Sensing, Artificial Intelligence, Classification, Human Vital Sign Detection

1. Introduction

In an emergency situation, it is important to make an initial assessment of a person's current health status in a short period of time in order to prioritise patients who require urgent care or conversely who are not in a critical condition. Such a classification is normally performed by humans using a triage process (Tam et al., 2018). There has been an increase in the use of robot and Artificial Intelligence (AI) based systems in healthcare; particularly since the COVID-19 pandemic (Bohr and Memarzadeh, 2020). Although the healthcare field was historically slow or hesitant to incorporate full robot or AI systems, the COVID-19 pandemic has resulted in many healthcare organisations incorporating the use of such systems, for example in room disinfecting, taking temperatures or acquiring COVID swabs (Lai et al., 2020).

Physiological monitoring is an important aspect of any triage or first responder robotic system. There are many physiological parameters that need to be considered, however, respiratory rate, heart rate and capillary refill time are amongst the most important. Changes in respiratory rate are a key indicator that a person's condition is deteriorating (Resuscitation Council UK (UK, 2021). Heart rate is measured as the number of times the heart beats per minute BPM. A normal heart rate for an adult in resting state is typically 60-100BPM although this may vary depending on age, weight, activity and fitness level. Normal breathing rates will vary depending on the age of the person. As adults, the rate may vary between 12-16 breaths per minute and increases with age, someone over 65 may have a rate of 12-18 breaths per minute and someone over the age of 80 may have a rate between 10-30 breaths per minute (Cook et al., 2021). Changes in respiratory rate are not just associated with respiratory conditions, they are a

good indicator that a patient is struggling to maintain homeostatic control (the body's internal environment) (Rolfe, 2019). Measuring RR involves determining how often the subject inhales in one minute and requires skilled personnel. If a person has shallow, rapid breathing or visibility is poor, it may be difficult to distinguish movement in the chest (particularly through clothing), there may be inaccuracies as it is often estimated or under reported.Challenges to measuring RR include drawing attention to the person's breathing and in doing so causes conscious control thereby disrupting automatic regulation which may affect their breathing pattern (Rolfe, 2019). CRT is a rapid, structured assessment of a person's circulatory system and can help determine their current state of health. CRT is dependent on the visual inspection of blood returning to the distal capillaries after they have been emptied by the application of external pressure (King et al., 2014). CRT is measured by pressing a thumb on the centre of the forehead (or sternum) for $\approx$ 5 seconds and then releasing it. For a healthy subject, skin colour should return to normal colour within 0.5-4.5 seconds although typically under 2 seconds (King et al., 2014). If the skin colour takes longer than 4.5 seconds to return to normal then the subject may be in shock.

The paper presents a robotic AI based triage system in the form of a fuzzy system which is designed to autonomously classify a human's health status based on their BPM, RR and CRT. The fuzzy system is trained on a large amount of synthetic data generated from discussions with a health professional. An effective AI based triage system would ultimately help free up time for medical professionals to focus on more complex duties and increase the safety of staff and patients with respect to COVID-19; automating the measurement of vital signs to inform the triage system would provide an ideal solution. This paper presents novel algorithms for measuring these vital signs using state of the art technology, showing how a robot may be endowed with a "first response" capability, for example in an emergency rescue scenario. The work outlined in this paper builds on the authors' previous work presented in (Kerr et al., 2015, 2018, 2019) for measuring BPM and RR with a robotic hand. In addition, the paper uses the method described in (Kerr et al., 2018) to compute CRT by using BioTAC sensors mounted on a Shadow Robot Hand combined with a simple imaging technique to calculate the time for the skin colour to resume normal colour. With a clear assessment of BPM, RR and a measurement of CRT vital signs being input into the fuzzy triage system, it is possible to

have a reliable and rapid indication of a person's current health and assess their need for emergency intervention. To validate the complete system, a pilot study classifying the health status of 12 subjects based on their vital signs is presented. The accuracy of the data collection and signal processing approach was evaluated on synthetic data, before using the vital signs collect from the 12 subjects to classify their current health status by inputting their vital sign readings into the fuzzy triage system. The results demonstrate that it is possible to accurately measure BPM, RR and CRT using a robotic system and using the data as inputs to the fuzzy system to classify a person's health using a fuzzy triage system.

The paper is organised as follows: Section 2 presents an overview of related research to automated triage systems, robotics in disaster zones and the methods and technology used for measuring human vital signs. Section 3 details the development of a fuzzy system intended to determine an overall state of health from synthetic data and subsequently from the vital signs measured from the participants. Section 4 outlines the data collection and algorithms developed for the measurement of BPM, RR and CRT in a pilot study of 12 subjects. Section 5 outlines the performance of the fuzzy triage system firstly when evaluated using synthetic data and secondly when using the aforementioned vital signs measured from human participants in the pilot study. Section 6 summarises the work and indicates plans for future work.

2. Background and Related Research

The rise of AI in the healthcare space has taken many forms, including key areas such as robotic assisted surgery, using machine vision and deep learning for medical image recognition and diagnosis, assistive robotics, neuroprosthetics and AI pre-qualification (triage) (Bohr and Memarzadeh, 2020). Although general triage systems covering all aspects of medical health may not yet be implemented, there has been increasing research in specific AI triage systems. Tam et al. (2018) implemented an AI triage system particularly for COVID-19 as it is recognised that hospitalisation is not often required for COVID-19 sufferers due to the majority of cases being mild. The digitally-automated pre-hospital triage system is capable of categorising a patient's severity and directing them to the appropriate healthcare setting. An Automated Triage System was developed by (Chong and Gan, 2016) with the aim of improving the service of an emergency de-

partment whilst reducing staff costs. Multiple sensors were utilised to read vital signs of the patient by a system incorporating an e-Health Kit, Arduino platform and a sphygmomanometer. Vital signs recorded blood pressure, temperature, RR and BPM. Additional information was manually entered via a Graphical User Interface (GUI) assisted by an assistant medical officer to detail attributes such as the patient's age, gender, current health and their main pain or complaint. Signal processing and a Random Forest machine learning technique (implemented in Matlab) was used to form the automated triage decision making algorithm. Generally, automated triage systems require the user to input details about themselves and their current pain/health. With the exception of systems such as the one developed by Chong and Gan (2016), automated triage systems rarely do any physical measurement of vital signs and even in this case the vital sign measurements required a medical assistant and further inputs to the system to classify the person's health from one of 6 possible outputs. Furthermore, the majority of automated triage systems are designed for use in clinical settings and would rarely be suitable for use in a disaster zone, in an emergency or in a patient's home on an ongoing basis. Therefore, a system that could carry out an assessment of a participant's vital signs and enable triage of victims would be extremely useful in a disaster, emergency or home scenario.

Research in robots being utilised in disaster zones has focused on being able to search the zone for survivors and determine safe routes to exit. Teleoperated robots that are able to move around disaster sites collecting and transmitting data have been a common focus for researchers. However, the methods and robots discussed in the literature to date are not capable of any physical interaction with humans when located. Furthermore, regardless of how a survivor is identified in a disaster zone there has been little work on the physical interaction with a human, for example, to release them from rubble or to use a robot to carry out a medical assessment (triage) of the survivor in situ. Samani and Zhu (2016) presented a mobile robotic ambulance called "Ambubot". The mobile vehicle is equipped with numerous sensors standard to that of a mobile robot such as two high resolution video cameras, sonar sensors and laser scanners. Although an effective and potentially very useful robot for rapidly deploying an automated external defibrillator (AED) to patients who have just had a cardiac arrest in the city, there were some constraints with the autonomous use and mobility. Furthermore, the robot requires a "smart

city" infrastructure in which to operate, to provide the locations of people in need of an AED. Murphy et al. (2013) investigated the use of robots to interact with trapped victims in terms of four different schemes: uni-directional video with no audio (from the robot at the victim back to responders), bi-directional video with no audio, uni-directional video (from robot to responders) with bi-directional audio and bi-directional video with bi-directional audio. Although communication was achieved between responders and a victim in a simulated building collapse, the authors identified key areas that require improvement for communication between victims and responders, including transparency of robot state and minimalistic interfaces. Even with this level of communication it would be difficult to carry out remote assessment of the victim's current health status, particularly if the victim is unconscious.

Regardless of the setting or how patient information is retrieved and inputted, in order to conduct an effective triage of a patient, vital signs signifying the patient's current health must be recorded. There are numerous key vital signs that can be measured from a human in order to ascertain their current health status. Some require more equipment and time than others but may provide more detail. For example, a complete 12-lead electrocardiogram (ECG) requires the connection of electrodes on the patient's limbs and the surface of the chest in order to measure the heart's electrical potential over a period of time and analysed in 10 second periods (a 10 second strip). Although this procedure would not be suitable for first response or in a disaster zone, it does provide a trained clinician with a large amount of information about the function of the heart's electrical conduction system along with heart rate and rhythm (Walraven, 2011).

Recently there has been much work done on the design and development of wearable sensors that are capable of monitoring vital signs. However, such sensors face numerous problems during testing such as intermittent skin contact, making it difficult to accurately monitor the aforementioned vital signs continuously. A sensor aimed at being integrated into a standard shirt was presented by Ramos-Garcia et al. (2016). Accurate measurements of breathing within a tolerance of 1 breath over a 10 seconds period was achieved and showed that the sensor could potentially be used as a means of continuously monitoring a person's RR. However, the assumption that a disaster victim would be wearing wearable sensors is dubious, and depends on these being present or indeed accessible. Therefore, one could not depend on wearable sensors as a means of

assessing, for example, the current health status of a trapped, unconscious person.

To date, the most common method used for measuring BPM and RR is the Doppler effect. Using microwaves and Radio Frequency (RF) to detect small movements such as heartbeat and respiration dates back to the 1970's (Lin, 1975). Gu and Li (2014) explain how the moving of the chest wall causes a Doppler shift and by analysing the phase information in the received radar signals it is possible to determine the RR and BPM. This approach to the measurement of RR and BPM has been heavily researched by many research groups, e.g (Choi and Kim, 2009; Lu et al., 2011; Iyer et al., 2013; Boothby et al., 2013) since the initial work by Lin (1975). Many radar-based approaches have inaccuracies, caused by spurious peaks often produced at harmonics and inter-modulation frequencies (Ren et al., 2015). Efforts have been made by Ren et al. (2015) to reduce these areas via the use of signal processing techniques. Accuracies of over 98% for heart rate in static mode and 94% in motion were obtained without producing spurious peaks, although tests were conducted on just one participant. More recently, Kuo et al. (2016) extended their previous work (Kuo et al., 2015) to develop a 60GHz complementary metal-oxide semiconductor (CMOS) based vital signs detection system using a single antenna. The clutter canceller which consisted of a Video Graphics Array (VGA) and a 360° phase shifter was reported to greatly increase sensitivity when detecting weaker human heartbeats and breaths. The vital signs could be read from a human up to 75cm away and the sensor was on a $2 \times 2mm$ chip which could eventually be installed onto a mobile robot for use in disaster zones. Although sensors utilising the Doppler effect are heavily researched and their accuracies for detecting human vitals are continuously improving, they would face difficulties when in uncontrolled environments as any other movement within the area would undoubtedly cause numerous artefacts in the signals received.

Another very popular method for measuring vital signs, particularly heart rate, is via camera equipment and image processing techniques. Tasli et al. (2014) use a standard off-the-shelf video camera to implement a remote photoplethysmography (PPG) based technique where variations in the colour of human skin were analysed for observing average heart rate. It was found that although acceptable accuracy was achieved in heart rates measured between 50-90 BPM with an average error of 2.9 and a standard deviation of 4.4. However, anything higher than 50-90 BPM tended to be

underestimated, with an average error of 4.2 and a standard deviation of 7.7. Additionally, it was found that changes in lighting dramatically affected the effectiveness of the method and that the success of this method requires training on a ground truth dataset of personal skin colour which may not always be available. Wu et al. (2012) also use a standard video camera and apply the Eulerian Video Magnification (EVM) technique to the video sequence. The authors recorded a video sequence of a human face and applied the EVM algorithm to each frame. They then amplified the resulting signal to reveal blood filling and leaving the skin, which is not visible to the human eye. Although a useful method to visualise and analyse human heart rate, this method struggles under changes in ambient lighting. Tran et al. (2015) presented a robust real time method that addresses issues relating to challenging environments for vision based heart rate measurements such as low illumination, movement of participants and complicated facial models that include beards and moustaches etc. The proposed method applies a combination of face detection/tracking and skin detection algorithms and the application of a finite state machine to reduce noise and construct a series of red, green and blue (RGB) images. The method is reported to perform well and is suggested for use in remote health care monitoring. However, as the focus of this work would be targeted for other areas outside of health settings where the environment will vary greatly, such as disaster zones; methods such as that of Tran et al. (2015) and other methods highlighted in this section would require further evaluation for extreme conditions. In contrast to using a standard camera, Gault and Farag (2013) use video frames from a thermal imaging camera to calculate heart rate from vascular mapping, blood perfusion and wavelet analysis. Various locations from the images, e.g. forehead, cheeks, chin etc., were evaluated for heart rate detection and an accuracy of $> 85\%$ was achieved when analysing the forehead region. However, like the other vision based heart rate measurement algorithms presented, this method may struggle in uncontrolled environments due to changes in ambient temperatures etc.

Other sensors that have been used to measure a heartbeat and RR include optical interferometers and vibration sensors. Although (Šprager et al., 2012) achieved an accuracy of $97.76 \pm 1.04\%$ for heart rate, these sensors are extremely sensitive and must be used in an embedded environment. Therefore, although they are useful for applications such as overnight monitoring of a patient's vital signs, they would not be use-

ful for measuring vital signs in emergency or disaster zones. Obo et al. (2017) use a vibration sensor in a bath to monitor heart rate due to the increased number of deaths in water in the elderly population. Their results are compared against the heart rate monitored by a conventional heart rate meter and the system was found to be very accurate. Although an effective system, it is specific to use within a bathtub and is unlikely to find widespread application. Furthermore, there has been a rise in smart watches such as Garmin, Apple and Fitbit watches being used to support health in everyday living. This is due to their potential to measure heart rate and analyse a user's activity (Blaine and Alexandria, 2016). Smart watches are capable of measuring heart rate and deriving which activity you may be completing from this reading, often coupled with the use of a built in accelerometer. Tedesco et al. (2019) conducted a study in users aged 65 and over to measure the accuracy of a number of devices. The devices tested were the Garmin VivoSmart HR+, Philips Health Watch, Fitbit Charge2, Omron HJ-72OITC, ActiGraph GT9X-BT and the Withings Pulse Ox (Tedesco et al., 2019). Measurements of steps taken, distance travelled and heart rate were taken during a walking test, household activities such as walking up and down stairs and carrying a box and sedentary activities such as writing, reading and playing cards. Watches were worn on both the dominant and non-dominant hands to evaluate any differences in accuracy. With regards to accuracies for all attributes measured; similar to previous studies, it was found that there was a large variation in accuracy, particularly for steps taken and BPM. It was reported that the devices were more inaccurate at step counting when the user was walking at a slower speed. The lowest Mean Absolute Percentage Error (MAPE) of 7.8% was found when the user was walking at $2k/m$ whereas there was a MAPE of 44.53% at speeds of $1k/m$. For tasks such as walking up and down stairs there was a difference in accuracy depending on which wrist the watch was worn on with a MAPE of 8.38–19.3% and 10.06–19.01% (dominant and non-dominant arm), respectively. Conversely, there was significant difference in accuracy between the dominant and non-dominant arm when measuring BPM. In line with previous studies the MAPE was relatively limited (between -3.57BPM and 4.21BPM); however, a single BPM measurement could be underestimated by up to 30BPM. Bent et al. (2020) investigated the reasons behind varying accuracies on wearable devices in order to concur or nonconcur with previous research which had stated that inaccurate BPM measurements occur up to 15% more frequently when

measured by watches worn on persons with dark skin as opposed to light skin (Fallow et al., 2013; Weiler et al., 2017). In their study of accuracy of wearable technologies across a full range of skin tones, Bent et al. (2020) found that where there was no statistically significant difference in accuracy across skin tones; there were significant differences between devices, and between activity types. In fact, the absolute error was was, on average, 30% higher during activity than during rest. They concluded that different wearable technologies including the Apple Watch 4, the Fitbit Charge 2 and the Garmin Vivosmart 3, to name but a few, were all reasonably accurate at resting and prolonged elevated BPM. However, when responding to changes in activity, differences in accuracy exist between devices. Maritsch et al. (2019) produced a method to improve the accuracies of wearable devices when measuring BPM by incorporating machine learning. Using methods such as explanatory and predictive modeling based on previous research; the authors found a statistically significant correlation between error in BPM measurements and the amount of movement completed by the wearer. Maritsch et al. (2019) show that the error rate can be minimised by incorporating contextual data such as the users movement when read from an accelerometer. Using a Deep Learning based Convolutional Neural Network (CNN) to predict the users activity based on accelerometer and BPM readings, the authors demonstrate that the error of smart watches can be reduced when measuring BPM. There was statistically significant correlation between medical heart monitor and the reading from a consumer smart-watch; with the root mean square of the successive differences (RMSSD) being improved from $r = 0.37, p =\leq 0.001$ before adjusting to $r = 0.58, p =\leq 0.001$ after adjusting. Although the accuracies of smart wearable devices are improving, they are related more to information for the user rather than being used by an external person or system to validate the users current health. In emergency or disaster zone, even if a person in need is wearing a smart watch which is accurately measuring their heart rate; this would not provide medical or rescue personnel with the information they require to triage the patient.

Together with the development of an effective automated triage system, this research focuses primarily on the use of force and tactile sensors for vital signs monitoring. Force or tactile sensing have not been significantly researched for this purpose. Mi and Nakazawa (2014) presented a thin multi-point polymer force/pressure sensor that they developed for pulse measurement from the radial artery on the wrist. The sensor is ex-

tremely thin measuring just 100 µm and it contains 25 sensing electrodes on a charged cellular polymer layer. The authors placed the sensor on the wrist of a human and visually assessed the detection of pulses against a physician's diagnosis in real time and reported that there was a strong correlation meaning the sensor is capable of sensing a heartbeat. Qian et al. (2011) also developed a tactile sensor for measuring pulse from indirect contact with an artery. The sensor is a tactile array consisting of six pieces of Polyvinylidene Fluoride (PVDF) films and is evaluated using a person's wrist, demonstrating effective measurement of pulse from the radial artery. A highly sensitive tunnelling piezoresistive tactile sensor was developed by Chang et al. (2016) for continuous blood pulse wave monitoring. The sensor proved effective at measuring pulse from a human's wrist. The work presented in the literature for tactile sensing focuses mainly on the development of application specific sensors in pulse measurement, however there is little research on using a multi-modal tactile sensor for BPM measurement on a triage robot.

3. Triage Health Status Classification

This section details the triage system that was designed based on a fuzzy system in order to determine a person's current state of health utilising measured vital signs, i.e., BPM, RR and CRT. In order to triage a patient's current health status, it is necessary to appropriately combine these vital signs to determine their overall health status. A fuzzy classification system (Cios, 2001) was determined to be the most appropriate approach due to it having fuzzy boundaries between classes enabling it to handle noisy and inconsistent real data. Algorithms capable of using data collected from a Shadow Hand equipped with BioTAC fingertip sensors to determine a human's BPM and RR, together with an approach to determining a human's CRT are presented in Section 4.

3.1. Fuzzy Classification Methodology

Fuzzy sets have the capability to model uncertainly and human linguistic descriptions within the reasoning process (Zadeh, 1965); In this work, a fuzzy classification algorithm was determined to be the most effective approach for classifying a human's health status based on the three aforementioned vital signs , as the fuzzy system accommodates the inherent uncertainties in measurements in a practical real-world context. Fuzzy

systems aim to model the human reasoning system, which Pal and Mandal (1991) state is approximate rather than precise in nature. Fuzzy logic systems have been used for numerous applications ranging from process control to medical diagnosis (Pal and Mandal, 1991; Ali et al., 2011; Dennis and Muthukrishnan, 2014; Nguyen et al., 2015). Other classification algorithms such as Artificial Neural Networks (ANN) and Support Vector Machine (SVM) were evaluated for classifying the measured vital signs data. However, due to the nature of vital signs data having overlapping boundaries for which a human is deemed "healthy", fuzzy logic approaches were determined to be the most suitable choice. A medical professional advised that there was a finite number of possible outcomes of health status when measuring vital signs in a disaster zone. These possible outcomes may be written as rules within a fuzzy logic system. The widely accepted Mamdani fuzzy system is suited to human style input (in this case a reading of a vital sign) and the output of a Mamdani-type fuzzy system can be easily transformed to a linguistic form in comparison with a Sugeno-type fuzzy system (Blej and Azizi, 2016). Therefore, a standard Mamdani fuzzy system (Mamdani, 1974, 1977) was selected. A Mamdani system defines a function, f, which generates numerical outputs $y = f(x)$ from numerical inputs, x, by using a set of IF/THEN rules (Zimmermann, 2001). In this case the numerical inputs are the calculated BPM, RR and CRT values and the numerical output refers to a specific health status. In order to allow for some cases where the numerical value for one or more of the vital signs may be borderline between two classes it is necessary to have some overlap in the membership functions. Furthermore, there may be cases where the person is extremely healthy and naturally has a lower BPM or RR. Gaussian membership functions have been found to perform well for similar applications due to their smooth curved edges and style of overlap (Hameed, 2011) and therefore will be used in the proposed fuzzy logic system.

The rules of the fuzzy logic system were determined based on the advice of a medical professional who determined possible status' of health based on the measurement of BPM, RR and CRT in an emergency scenario and by referencing (Royal College of Physicians of London, 2012), which is the UK National Health Service (NHS) standard for the assessment of acute illness and severity. Graphs displaying the membership functions for each input are shown in Figure 1. The aim is to determine a participant's health by monitoring their BPM and RR over a 60 second period

and taking one measurement of their CRT rather than continually monitoring their vital signs over a longer period of time. Therefore, there are 9 possible outcomes that can be determined in an emergency type scenario. These are shown in Table 2. The nine outcomes were represented by triangular membership functions. As there were possible combinations that would not represent one of the nine possible diagnoses', there was a tenth membership function included for all non-classified combinations, including unrealistic values of the vital signs that may for example have been caused by sensor error. A graph displaying the output membership functions is shown in Figure 2.

Table 1: Details of the Input Membership Functions

Input	**Membership Function**	**Range**
BPM	Zero	0-2
	Low	1-63
	Normal	50-110
	High	97-240
RR	Zero	0-2
	Below Average	1-13
	Normal	7-25
	Above Average	20-80
CRT	Normal	0-2.5
	Prolonged	2-11
	Infinite	10-60

The MATLAB Fuzzy Logic Toolbox (2013) was used to develop the fuzzy algorithm, which includes five defuzzification methods. As it is required that the most likely output from the combination of vital sign inputs is selected, the 'centroid' defuzzification method was used. This method returns the centre of the area underneath the curve of the fuzzified outputs. It is the most common and effective method for converting the result to a crisp output (Naaz et al., 2011). The returned centroid value is rounded to the smallest integer greater than or equal to the centroid value. Table 2 shows pseudo code of the fuzzy rules related to the membership

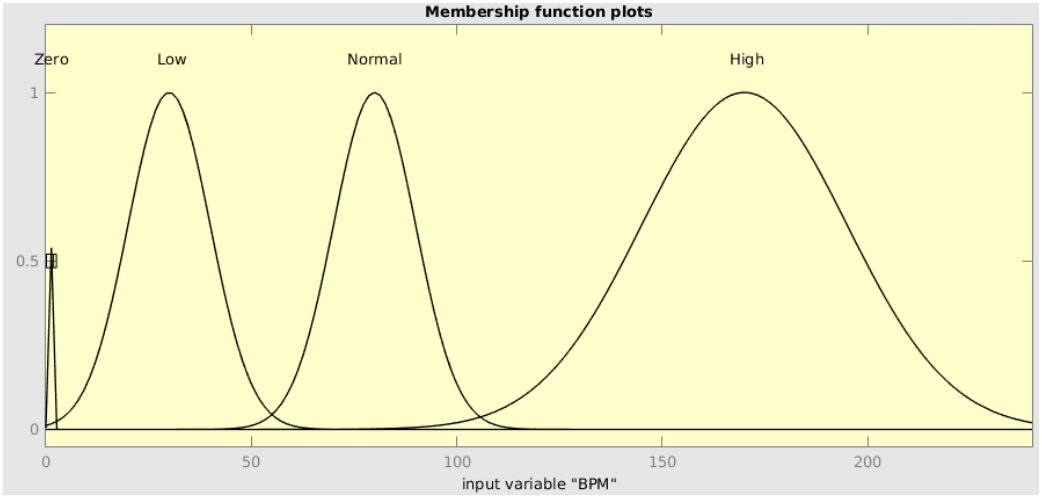

(a)

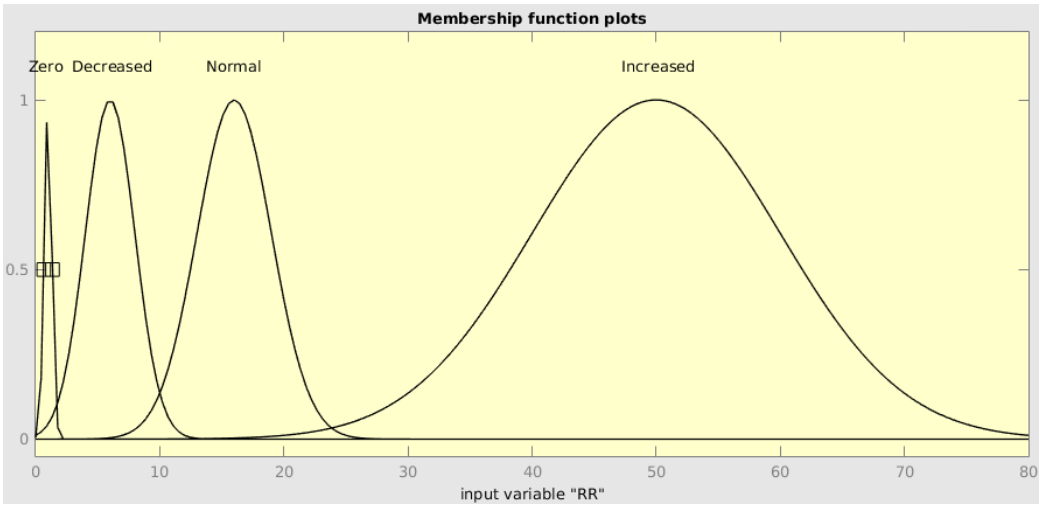

(b)

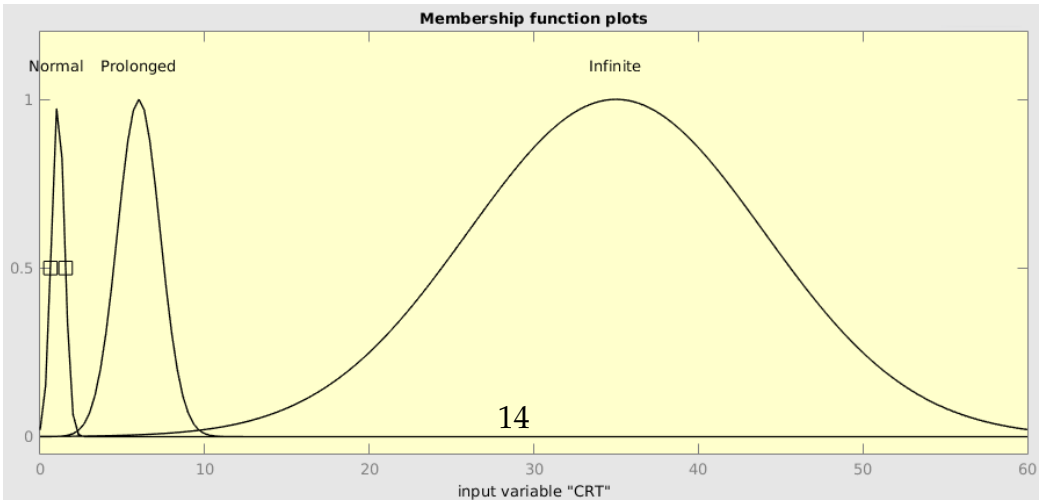

(c)

Figure 1: Graphs displaying membership functions for a) BPM; b) RR; c) CRT

functions outlined in Table 1, the output integer related to each rule and a description of what each output represents in relation to the participant's health status.

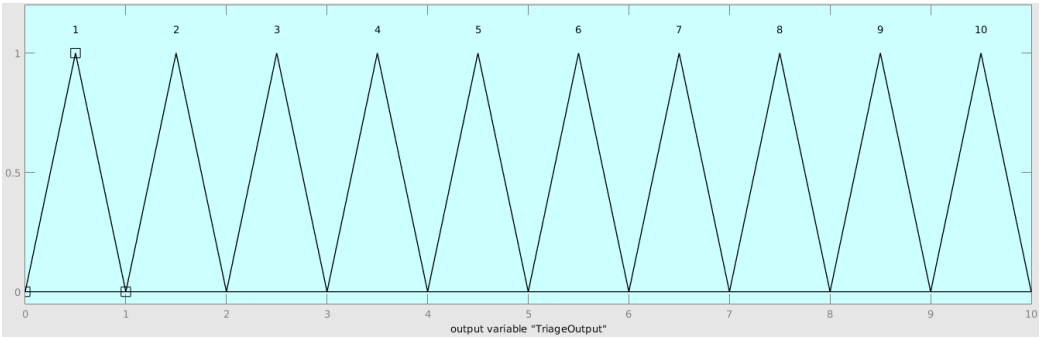

Figure 2: Graph showing the membership functions for the outputs of the Fuzzy System

Table 2: The Outputs of the Fuzzy Logic System

Fuzzy Rule	**Output**	**Description**
If (BPM is Normal) and (RR is Normal) and (CRT is Normal)	1	Healthy
If (BPM is Low) and (RR is Normal) and (CRT is Normal)	2	Heart Block / Fit
If (BPM is Low) and (RR is Below Average) and (CRT is Normal)	3	Unconscious / Sleep
If (BPM is Normal) and (RR is Above Average) and (CRT is Normal)	4	Acute Deterioration
If (BPM is High) and (RR is Above Average) and (CRT is Normal)	5	Pain / Anxiety
If (BPM is High) and (RR is Below Average) and (CRT is Normal)	6	Central Nervous System (CNS) Depression / Traumatic brain injury (TBI) (Bang on Head)
If (BPM is High) and (RR is Above Average) and (CRT is Prolonged)	7	Hypovolemic shock / Open Wounds / Bleeding Out
If (BPM is Low) and (RR is Below Average) and (CRT is Prolonged)	8	Critical (close to death)
If (BPM is Zero) and (RR is Zero) and (CRT is Infinite)n	9	Dead

4. Pilot Study

This section outlines the pilot study which involved collecting vital signs from 12 subjects using a robotic system. These data were subsequently used as input to evaluate the effectiveness of the fuzzy triage system (outlined in Section 3) with real medical data. The various methods used to determine the BPM, RR and CRT are presented and discussed. As some aspects of the algorithms for RR are similar to that of the BPM then these two methods are outlined in Section 4.1 and the CRT method is briefly outlined in Section 4.2; more detail on this method can be found in (Kerr et al., 2018).

4.1. Determination of BPM and RR

We utilise the Shadow Hand equipped with three first generation BioTAC™ sensors from Syntouch® to collect BPM and respiratory information from subjects (Kerr et al., 2019). The Shadow Hand has 21 degrees of freedom and hence can replicate the motions required to measure BPM from a subject's wrist and sense movement in their chest. Figure 3(a) illustrates the Shadow Hand while Figure 3(b) shows the cross section of the BioTAC sensors.

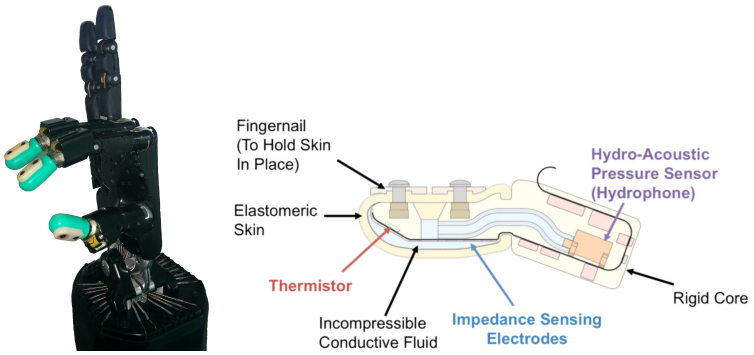

(a) (b)

Figure 3: (a) Image of The Shadow Hand with three mounted BioTAC Fingertip Tactile Sensors (b) Cross Section View of BioTAC Fingertip Tactile Sensor (Syntouch, 2013)

The first generation BioTAC is a tactile sensor which is shaped like a human fingertip and is liquid filled, giving it similar compliance to a human fingertip. It measures force applied across an array of 19 electrodes,

absolute fluid pressure (PDC), dynamic fluid pressure (PAC), static temperature (TDC) and thermal flow (TAC). We use vibration data to measure BPM while measuring breaths is achieved using vibration and temperature data, used concurrently to ensure algorithm robustness. In the case of BPM measurement, contact with a human wrist allows for sensing vibration caused by blood flow through the radial artery and contact with the chest allows for sensing vibration signals caused by the lungs inhaling and releasing air when breathing. In all cases, this work uses a lowpass filter as a first stage of noise reduction and utilises wavelet algorithms as a second stage of noise reduction, thus improving the overall noise reduction in the BPM and respiratory rate waveforms, similar to the method outlined in (Kerr et al., 2015, 2019). A further smoothing algorithm based on lateral inhibition is also considered in this paper to evaluate if it is effective as a third stage of smoothing.

4.1.1. BPM and RR Data Collection

BPM and RR data were collected from 12 human participants, all of whom were volunteers from within the Intelligent Systems Research Centre (ISRC) at the Ulster University (UU) Magee Campus. All participants were healthy 18-65 year olds. A medical professional oversaw the procedure and measured each participant's BPM and respiratory rate in each experiment as ground truth data to verify the accuracy of the novel artificial system approach developed.

To measure BPM, each participant was seated in front of the robot hand and asked to place their (sleeveless) left wrist facing upwards into the robot hand, as illustrated in Figure 4(a). Using the BioTAC fingertip the force applied is measured and once sufficient contact is made with the wrist by the first finger (FF) and middle finger (MF), the fingers stop and the system records the PAC data. The Shadow Hand applied a safe level of force similar to that which a human would apply. As the fingertips are soft and warmed to approximately the same temperature as a human fingertip they did not cause any pain or discomfort to the participants. Three datasets of 120 seconds each were collected with a short break in between each one. The individual was at rest in each case.

In order to determine the RR of the participant, contact with the chest of each of the 12 participants was made using the Shadow Hand (see Figure 4(b)). The BioTAC sensors were closely monitored to ensure sufficient contact was made with the chest. The required force was determined us-

ing the ATI Nano17 6-axis Force/Torque (F/T) Sensor (ATi, 2017) measuring the force that a medical professional applies to a human chest when attempting to measure respiratory rate. In this case static vibration data (PDC) were used to identify the movements of the chest wall more effectively than PAC. Furthermore, as breathing can cause a lot of added artefacts and noise, the thermal conductivity value (TAC) was measured along with vibration data. As the chest wall rises during breathing, the skin of the participant pushes against the inside clothing hence the thermal conductivity value (TAC) fluctuates as the temperature and friction changes. Therefore, both TAC data and PDC data were recorded to assess respiratory rate in order to add robustness to the algorithm.

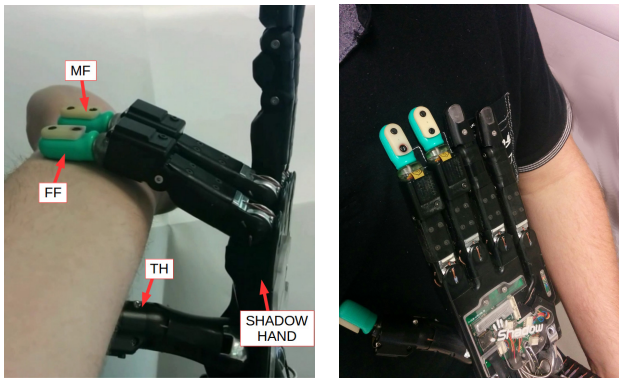

(a) (b)

Figure 4: (a) Image showing the Shadow Hand taking the participant's BPM (b) Image showing the Shadow Hand resting on the participant's chest to measure RR

4.1.2. Waveform Pre-processing

Discrete wavelet transform (DWT) algorithms with two wavelet functions, namely Haar and spline (SPL) (Luo et al., 2006) and various levels of decomposition were evaluated. The Haar wavelet is a wavelet family compiled of a sequence of rescaled "square-shaped" functions and is the simplest possible wavelet (Misiti et al., 2007). The SPL wavelet function used in the DWT wavelet algorithm is the B-spline of order 2, namely the quadratic B-spline (Misiti et al., 2007). It was empirically found that a DWT wavelet algorithm with a SPL wavelet filtering algorithm and a wavelet decomposition value of 5 is the most effective algorithm provid-

ing smoothing without loss of information. Therefore, this was applied to all waveforms collected for BPM and respiratory rate.

Reichardt and MacGinitie (1962) initially studied the use of lateral inhibition in various neural networks and since then there has been continuous interest in these networks, particularly in the field of sensory analysis. The method is capable of highlighting the peaks in a waveform and suppressing any data points that were not considered to be part of a peak by using a linear threshold output function with the lateral inhibition neural network. As lateral inhibition is used to emphasise peaks in data, the data are inverted for trough detection cases. In this work, we applied a Butterworth infinite impulse response (IIR) filter with a cut off frequency of 10Hz throughout the BPM and respiratory experiments presented. This is followed by a lowpass filter known as the scaling function, first introduced by Mallat (1989), designed such that its spectrum fits in the open spaces left by the wavelets. Finally lateral inhibition is applied as a third stage of smoothing and is compared with using only the low pass filter and the wavelet algorithm as a two-stage smoothing approach.

4.1.3. BPM and RR calculation

By identifying and calculating the number of troughs (or peaks) in a 60 seconds window of the BPM waveform, the participant's BPM can be calculated. However, as breathing is calculated by analysing the PDC and TAC readings from the BioTAC, i.e. the pressure and thermal conductivity, it was evident upon visual inspection following the first two stages of filtering and smoothing that in these waveforms peaks are more prominent than troughs. This is to be expected as when the chest wall rises (to accommodate an intake of air) the skin presses firmly against the clothing increasing thermal conductivity which is measurable using the BioTAC fingertip. Therefore, by identifying the number of peaks (breaths taken) within a 60 second period of the respiratory data the participant's RR can be calculated. We detect salient troughs and peaks using the function "peakdet" in MATLAB and the function uses a threshold (default 0.5).

Due to the range of variance within the datasets for each modality (i.e. PAC, PDC and TAC), the default threshold was not adequate for accurately differentiating all the troughs and peaks from within the various waveforms. Therefore, a dynamic threshold was required, similar to that in (Kerr et al., 2019), but suitable for BPM and RR data. Two thresholding approaches were evaluated, one semi-automatic and one fully automatic.

The semi-automatic approach enabled calibration per participant for improvement of accuracy as the troughs and peaks in the graphs vary in terms of how prominent they appear from their surrounding values across each participant. This avoids any outstanding residual noise from being detected as a trough or peak. As the troughs or peaks are detected with respect to the resting waveform the calibrated dynamic threshold (dt_m) is computed for each modality per participant using the standard deviation and is given by:

$$dt_m = x \times \sigma \tag{1}$$

where x is a factor calibrated for each participant per modality, and σ is the standard deviation of the waveform. A range of values of x were used and tested for each modality and manually calibrated for each participant to determine the optimal threshold enabling accurate troughs and peaks detection representing heart beats and breaths respectably.

The fully automatic thresholding approach was implemented based on the technique used by Jacobson (2001) in his approach for automatic peak detection in ECG signals. The approach considers the fact that the slope of a leading edge of a peak is positive. It computes the sample derivative and those greater than zero are classified into two clusters, a peak slopes cluster and a cluster of remaining values in the waveform. Using a nearest neighbour style approach to separate the two clusters, each data point in the waveform is considered in turn and assigned to the cluster whose mean is closest in value to the data point. Once this is completed for all data points, new means are calculated for the two clusters and the process is completed again where each data point is classified into the two clusters. At each iteration the difference between the means of the two clusters is calculated and the process continues until the difference is below a specified termination value. Due to the nature of the data analysed and considering how noisy it can be, the algorithm is designed to continue until the difference between the two means is less than 1 in the expectation that this would produce the most accurate threshold for each waveform, resulting in accurate peak detection. The results are presented for algorithms using the semi-automatic approach and the fully automatic approach in order to evaluate which method is most accurate.

The Pulse to Pulse Interval (PPI) and Breath to Breath Interval (BBI) calculation can be determined in a similar way to that described above,

and therefore the reader should refer to (Kerr et al., 2015, 2019) for further details if required.

4.2. Determination of CRT

Measurement of CRT can be achieved by determining the change in skin colour on a human subject resulting from a press action to the centre of the participant's forehead. For this we used a combination of the BioTAC fingertip on the Shadow Hand and a small 1000 Television Lines (TVL) camera illustrated in Figure 5.

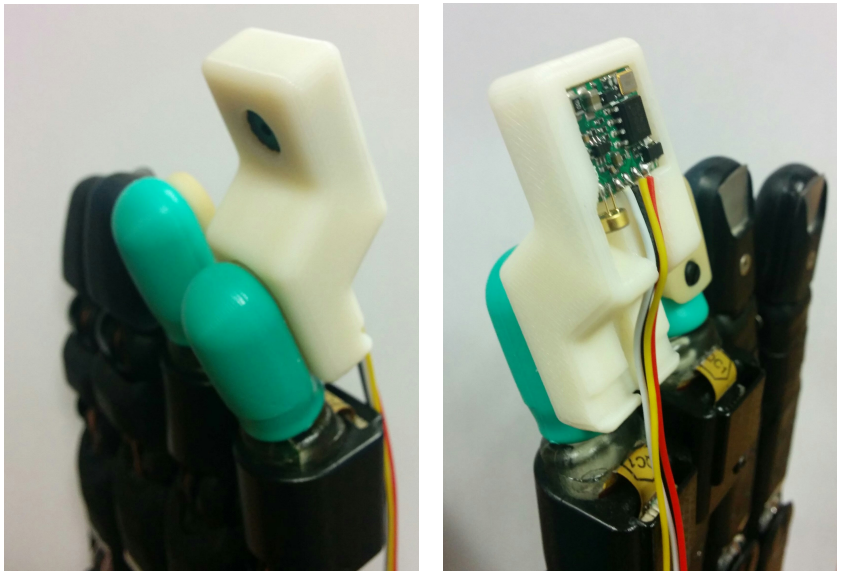

(a) (b)

Figure 5: Images showing the customised camera mount on the Shadow Hand from (a) the front and (b) the rear

Data were collected from 12 healthy participants, as outlined in Section 4.1.1. In order to overcome the well known difficulties of ambient light, data were collected at different times of the day for different participants.

A novel method for identifying the duration of the capillaries refilling was developed by analysing the gradient changes in the graph of red pixel values, whilst ensuring that gradient changes not relevant to the capillaries refilling were ignored. A dynamic threshold was calculated and

utilised for the analysis of each dataset to remove noise and determine significant gradients. The threshold for identifying significant positive gradients was set as the mean of the positive gradients and the mean of the negative gradients was used as the threshold for identifying significant negative gradients. For further details on this approach the reader should refer to (Kerr et al., 2018).

4.3. Evaluation of Measured Vital Signs

In this section, results are presented for the determination of participants' BPM and RR together with the calculation of the PPI and BBI for each participant in Section 4.3.1. Furthermore, results for the CRT calculated for each participant are also presented in Section 4.3.3.

4.3.1. BPM and RR Results and Discussion

Results are presented for BPM and RR identified from waveforms following two stages of smoothing. A third stage of smoothing using lateral inhibition neural networks was also evaluated and the results for BPM and RR following this extra stage of smoothing are also presented for comparison. The results are evaluated against the manual measurement (ground truth) of each participant's BPM measured by a medical professional. Results are also presented for the calculation of the PPI and BBI. For comparison, the algorithm's performance is also evaluated against a modern off the shelf light-based BPM measurement device. During data collection, the participant's BPM was also measured using an Android smart-phone application called "Heart Rate Monitor" (Mellado, 2013). The smart-phone application requires the user to place their index finger against the camera lens of the phone. It then analyses the input from the camera feed, detecting the slight changes in red colour to identify pulses. The algorithm applies band pass filtering to the signal and then begins a sliding window approach to analyse the signal. Within the sliding window a Fast Fourier Transform (FFT) is applied to the signal followed by a peak detection algorithm in which it classes each peak as a pulse. A smoothing algorithm is then applied to the signal thus it is displayed as a smooth waveform with minimal noise. Similarly, it was found that applying the low bandpass Butterworth IIR filter to the raw PAC, PDC and TAC data collected using the BioTAC, reduced noise and smoothed the waveform to a level that may in some cases be sufficient to clearly identify peaks and troughs. This can be seen in Figure 6(a) which shows an example of the raw PAC

data collected from the wrist of one of the participants and the filtered data following application of the IIR filter, in this case from participant 3. A similar smoothing is achieved with the application of the IIR filter on the PDC and TAC data.

Application of the second stage of filtering, namely the DWT noise reduction process, to the raw data successfully further removed noise, smoothed and normalised the waveform to a level that would allow for successful trough and peak and therefore BPM and breath detection. The data contained significantly less noise compared with using only a low pass filter. For example, this is evident in Figure 6(b) which shows the PAC data following the application of the DWT noise reduction algorithm where the data are clearly less noisy than the raw or single stage filtered data. As described in Section 4.1.2, lateral inhibition was also applied to each dataset to evaluate if it would improve the accuracy of BPM and breath detection in their respective datasets. It was found that the application of the lateral inhibition algorithm does not reduce noise any further than the two stage filtering process.

The trough/peak detection algorithm with the semi-automatic thresholding method has proven to work well for BPM and breath detection enabling accurate BPM calculations. Figure 7(a) shows the troughs (representing BPM) detected by the trough detection algorithm using the semi-automatic thresholding method, highlighted by blue stars. Tuned threshold values for each participant were empirically found and ranged from 0.090-1.323 (representing value x in equation 1). Figures 7(b) and 7(c) show the breaths detected represented by peaks in the PDC and TAC waveforms respectively. It can be seen in Figure 7 that the trough detection algorithm detects the majority if not all of the troughs or peaks in all cases when the thresholds are semi-automatically calculated with manual fine tuning. Tuned threshold values for each participant per modality were empirically found and ranged from 1.000-2.545 for PDC and from 0.6-2.5 for TAC (representing value x in equation 1). However, it can also be seen in Figure 7(b) that there can be some instances where it would be expected that a peak would be detected as a breath but it hasn't been detected (one such instance is highlighted by the green circle). This is an example of where the points on either side of the peak are just below the threshold for difference and therefore it is not classified as a breath. It is due to borderline cases like this that some of the calculated BPM and RR may be marginally incorrect when compared with the readings measured by a medical professional.

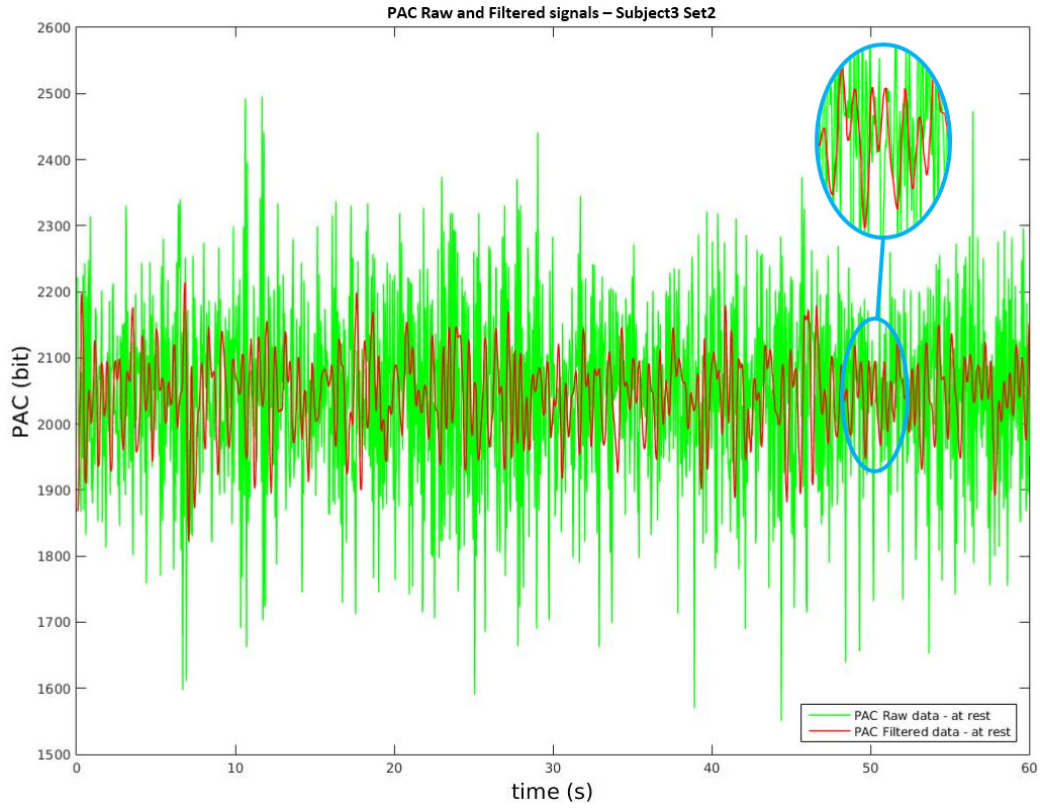

(a)

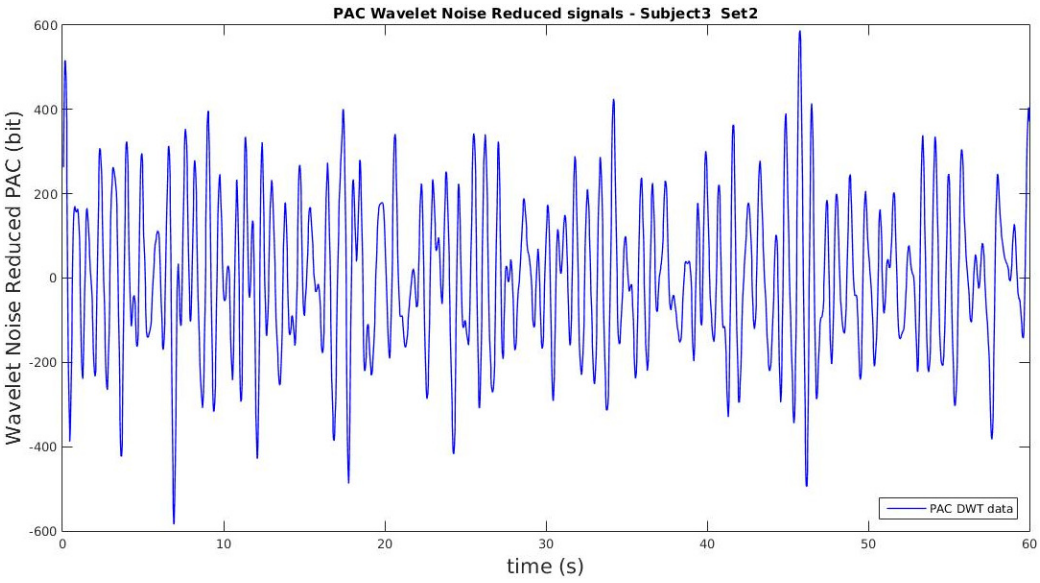

(b)

Figure 6: Graphs showing (a) the raw and low pass filtered PAC data collected from participant three's wrist and (b) the PAC data after wavelet smoothing was applied.

However, the benefit of this approach is that the algorithm does not detect all peaks or troughs in the waveforms particularly when a series of these occur and would clearly be an incorrect representation of BPM or breaths. An example of this is highlighted by the purple circle in Figure 7(c) where there are three obvious peaks however they are correctly not considered as breaths by the algorithm.

The trough/peak detection algorithm with fully automatic thresholding method has been shown to be less effective than the semi-automatic thresholding method, proving to be over sensitive when detecting troughs and peaks. An example of this is demonstrated in Figure 8 where there are too many peaks detected as breaths particularly in a short space of time, highlighted by the green circles.

Results from analysis of the data for the BPM can be seen in Table 3. The average of the absolute difference between the calculated BPM and the actual BPM measured by a medical professional is shown for each method. The minimum and maximum difference from the actual BPM that each method measured is also shown in Table 3. A calculation of the accuracy of each method when classifying if the participant was bradycardic, normal or tachycardic is also presented in the "Correct Class (%)" row of Table 3. Results for the two stage filtering approach with semi-automatic thresholding are presented in the column labelled "2SFS" (2 Stage Filtering Semi-automatic). Results for the two stage approach with fully automatic thresholding are presented in the column labelled "2SFF" (2 Stage Filtering Fully-automatic). Results for the three stage approach (i.e. using low pass filtering, DWT and lateral inhibition smoothing) with semi-automatic thresholding are presented in the column labelled '3SFS" (3 Stage Filtering Semi-automatic) and the results for the three stage approach with fully automatic thresholding are presented in the column labelled '3SFF" (3 Stage Filtering Fully-automatic). The results using the Android smart-phone application (Mellado, 2013) are also presented in the column labelled 'SPA" (Smart Phone Application).

It can be seen from Table 3 that the best performing approach is the two stage filtering/smoothing approach with the semi-automatic thresholding algorithm as it allows for calibration to be tuned per participant. This approach achieved an average of just 1.47 BPM difference from the actual measured BPM across all datasets. In fact, this method calculated the exact BPM in 13 instances out of the 36 datasets. This approach also correctly determined if the participant's heart rate was classified as brady-

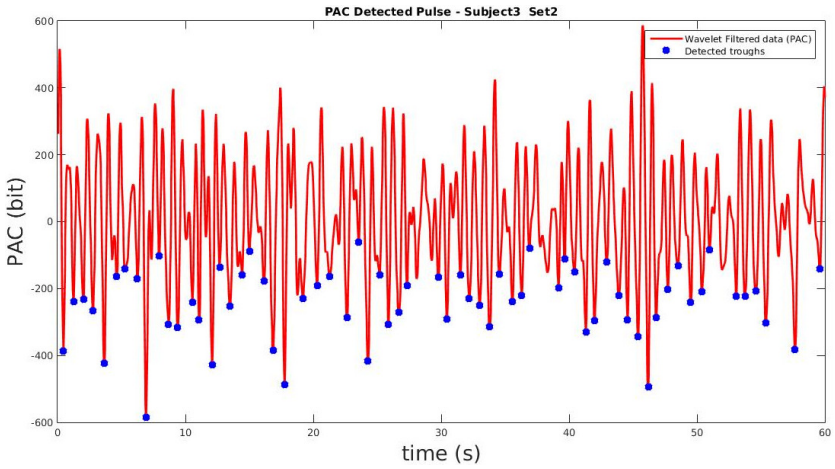

(a)

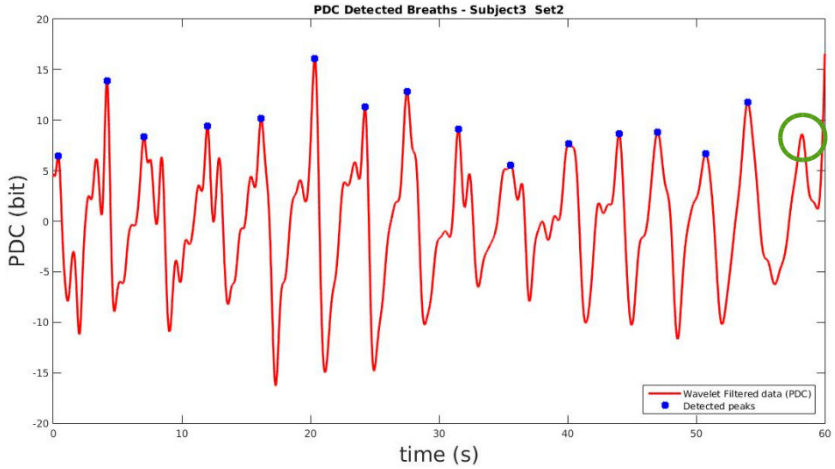

(b)

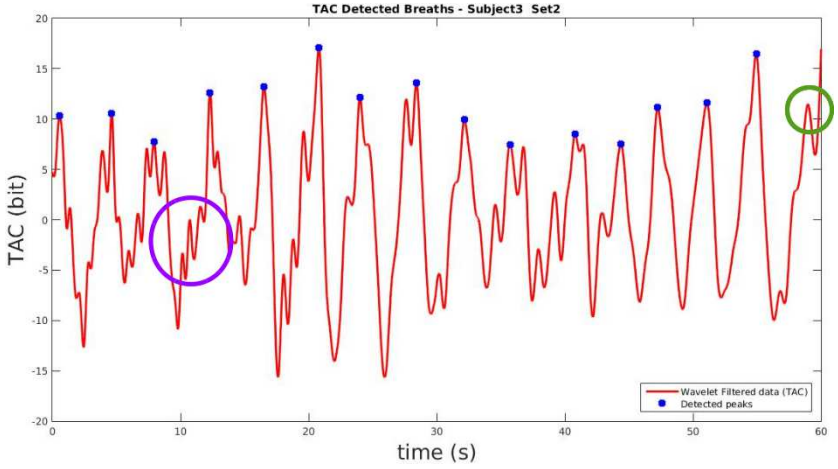

(c)

Figure 7: Graphs showing (a) the detected troughs in the PAC data relating to BPM, (b) detected peaks in the PDC and TAC data (c) representing breaths.

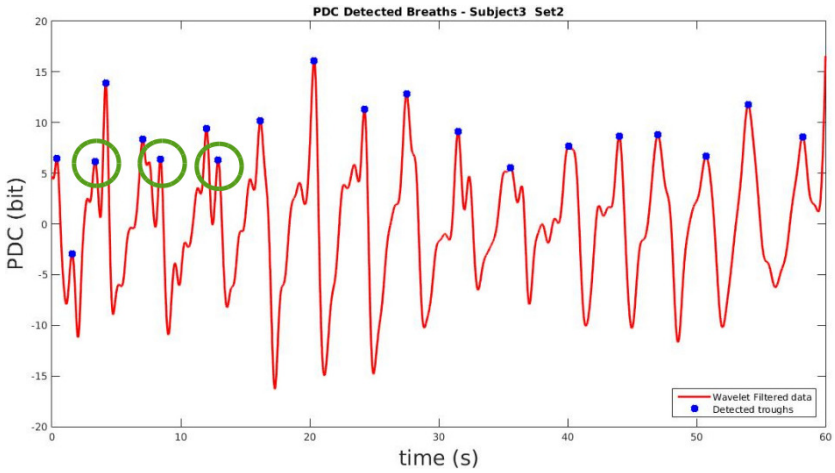

Figure 8: Graph showing the peaks detected in the PDC dataset with the use of fully automatic thresholding

Table 3: Table comparing the BPM experimental results

Difference From Actual	**2 Stage Filtering Semi-automatic (2SFS)**	**2 Stage Filtering Fully-automatic (2SFF)**	**3 Stage Filtering Semi-automatic (3SFS)**	**3 Stage Filtering Fully-automatic (3SFF)**	**Smart Phone Application (SPA)**
Average	1.47	4.28	2.19	6.22	16.47
Min.	0	0	0	0	1
Max.	13	14	14	17	53
Correct Class (%)	97.22	97.22	97.22	100.00	91.67

cardic ("B"), normal ("N") or tachycardic ("T") in 97.22% of cases which collates to 35 of the 36 datasets.

The three-stage filtering/smoothing method also achieved 97.22% accuracy when classifying the heart rate. This method was slightly less accurate than the two-stage approach when measuring the BPM achieving an average of 2.19 BPM difference from the actual measured BPM. It can be seen from the results presented in Table 3 that the addition of the lateral inhibition smoothing for a third stage of filtering/smoothing does not provide any further benefit in improving the overall accuracy of BPM calculation, however it is still a viable approach which produced accurate results for classifying a heart rate.

The results presented in Table 3 show that the fully automatic thresholding approach did not produce results of similar accuracies to those produced by the semi-automatic thresholding method. However, it can be seen that although the algorithm did not determine the exact BPM, it achieves similarly high accuracies when classifying the heart rate. Therefore, it could be a useful approach to rapidly determine an estimate of the status of a person's heart rate in an emergency scenario.

Analysis of the results for the calculated RR can be seen in Table 4 and Table 5. The average, minimum and maximum of the absolute difference between the calculated RR and the actual RR measured by a medical professional are shown in Table 4 and Table 5 for each method when using PDC and TAC respectively. A calculation of the accuracy of each method when classifying if the participant had a slow, normal or fast breathing rate is also presented in the "Correct Class (%)" rows of Table 4 and Table 5. The same labelling for column headings as Table 3 apply to Table 4 and Table 5.

Table 4: Table comparing the RR experimental results with PDC data

Difference From Actual	**2SFS**	**2SFF**	**3SFS**	**3SFF**
Average	0.56	7.00	0.92	10.97
Min.	0	0	0	0
Max.	4	28	4	32
Correct Class (%)	91.67	41.67	91.67	22.22

Table 5: Table comparing the RR experimental results with TAC data

Difference From Actual	**2SFS**	**2SFF**	**3SFS**	**3SFF**
Average	0.72	5.39	0.83	11.89
Min.	0	0	0	1
Max.	7	24	4	21
Correct Class (%)	72.22	47.22	83.33	11.11

It can be seen from Table 4 and Table 5 that the best performing method was the two stage filtering/ smoothing with semi-automatic thresholding, as was the case with the BPM calculations. It has been proven that both the PDC and TAC data have performed similarly well. In the majority of cases the classification of the RR when using PDC and TAC was classified in the correct class. It is evident from the results in Table 4 and Table 5 that the fully automatic thresholding approach was not suitable for classifying the RR of the participants. It is also evident that although the addition of the third smoothing algorithm, lateral inhibition, did not lower the accuracy of the RR calculations, it also did not improve the calculations or classifications and therefore is not worth extra computation time, as is the case when calculating the BPM.

4.3.2. PPI and BBI Calculation and analysis

The pulse to pulse (PPI) and breath to breath (BBI) intervals were successfully calculated between individual troughs detected and the average interval of troughs detected within a sliding window for each dataset. Analysing these values of PPI and BBI can determine if a participant's pulse was in sinus rhythm or a form of arrhythmia and if a participant's breathing is occurring in a regular rhythm. Due to the nature of the data being collected and the noise levels present in the data it is expected that the intervals between detected heart beats and breaths will not be exactly equal from pulse to pulse or breath to breath. This is similar to real life when medical professionals are reading BPM and RR manually. They would not be capable of detecting minor sub second differences in the intervals between pulses or breaths, rather assessing for a change to pulse or breathing intervals representing an irregular or stressed heart or breathing

rate, hence the inclusion of the 25% tolerance for the interval times.

Table 6 shows an analysis of the PPIs calculated using each method. The number of instances where the calculated interval between pulses that were within the acceptable 25% tolerance of the average interval was identified for each method. The average, minimum and maximum percentage of intervals within the tolerance across all datasets for each method are shown. Table 7 presents the average, minimum and maximum percentage of the calculated intervals between each detected breath that were within the 25% tolerance of the average interval using PDC data and TAC data. The column headings labels have the same meanings as outlined previously for Table 3. It is evident from Table 6 that in some cases quite a few of the intervals are not within the tolerance which could represent an irregular pulse; however, none of the participants had an irregular pulse. As accuracies are analysed in the scale of tenths and hundredths of a second for these measurements it is difficult to put a binary classification of regularity for a pulse waveform. However, in some instances the majority of pulse intervals are within the tolerance, up to 98.88% is achieved by all methods. Similar to the method for calculating BPM, it is evident from Table 6 that the most accurate method for assessing the interval between each heart beat is the two stage filtering/smoothing approach with semi-automatic thresholding.

Table 6: Table comparing the PPI experimental results

Percentage within tolerance	**2SFS**	**2SFF**	**3SFS**	**3SFF**
Average	73.56	72.07	68.96	65.68
Min.	38.16	38.67	33.75	34.94
Max.	98.88	98.88	98.88	98.88

Due to the nature of the breathing data collected and the fact that there is a lot fewer occurrences of a breath in one minute than a heart beat, it can, in some instances, be less challenging to calculate an accurate interval between each breath than between each heart beat. Table 7 shows that assessment of the intervals between breaths can be very accurate when using the two stage filtering/smoothing approach with semi-automatic thresholding. With similarly accurate results being obtained using PDC data and the highest accuracy of 100.00% was obtained using PDC data as

shown in Table 7, it is proven that, either PDC or TAC data can be used for analysis of breath intervals.

Table 7: Table comparing the BBI experimental results

Data type	Percentage within tolerance	2SFS	2SFF	3SFS	3SFF
PDC	Average	68.92	51.51	67.63	30.33
	Min.	23.53	33.33	41.18	9.09
	Max.	95.45	77.78	100.00	69.70
TAC	Average	71.87	46.40	69.17	26.84
	Min.	37.50	26.83	19.05	9.09
	Max.	91.67	70.73	95.45	66.67

4.3.3. Evaluation of CRT Measurement and Discussion

This section presents an overview of the results for the experiments calculating the CRT from 12 healthy human participants of varying skin tone. For complete analysis of the results please refer to (Kerr et al., 2018). As there is no medical method for calculating a precise value of CRT, a medical professional verified that all participants were healthy and their CRT was below the expected duration of 2 seconds. Table 8 presents the minimum, maximum and average CRT for each participant. Using a maximum of 3 datasets per participant, the number of sets in which CRT was correctly calculated and took less than 2 seconds is also presented.

As the participants are all healthy subjects, 2 seconds is used as the threshold to determine a status of healthy, in shock or critical condition (Royal College of Physicians of London, 2012). Table 8 indicates an accuracy of 89% (32/36 datasets correctly determined).

It should be noted that for robustness, the participants were of varying skin colour (Black, Indian and Caucasian), demonstrating that the algorithm works regardless of skin colour.

Table 8: Table outlining the calculated CRT experimental results

Participant	**Average (*s*)**	**Min (*s*)**	**Max (*s*)**	**Sets** $< 2secs$
1	0.976	0.909	1.082	3
2	1.111	1.010	1.309	3
3	0.739	0.551	0.842	3
4	3.772	1.091	6.983	1
5	0.869	0.681	0.995	3
6	1.001	0.940	1.121	3
7	1.421	1.085	1.877	3
8	2.362	0.978	5.019	2
9	1.715	0.759	3.554	2
10	0.988	0.908	1.121	3
11	1.117	0.976	1.222	3
12	1.081	0.875	1.264	3

5. Fuzzy Classification Results and Discussion

This section presents the results from the evaluation of the fuzzy triage system. The results from the system when evaluated on synthetic data are presented first followed by the results of teh fuzzy triage system when evaluated using real patient data collected during the pilot study.

5.1. Fuzzy Classification Results and Discussion - Synthetic Data

To suitably evaluate the fuzzy logic classifier, synthetic data were used to appropriately represent all nine possible outcomes; enabling a thorough evaluation of all possible outputs from the fuzzy system. The synthetic data consisted of 10,000 datasets of BPM, RR, CRT for each possible output. In consultation with a medical professional, the values for BPM, RR and CRT were generated within the ranges for each sign as outlined in Table 1 using a pseudo-random number generator. For example, a range of values representing BPM were pseudo-randomly generated over the intervals 1-63, 50-110 and 97-240 to represent low, normal and high BPM respectively. There was a total of 90,000 (10,000 x 9) datasets created, representing all possible outcomes and ensuring that there were sufficient datasets which included values in the overlapping areas of the

membership functions. As the synthesised dataset contained combinations of pseudo-randomly generated data to fulfil one of the nine possible outcomes, it was possible that it would differ from the real collected data as there could be misreadings (due to sensor error) in the real data causing a combination that was not necessary to be included within the synthetic dataset. Furthermore, the synthetic dataset was generated based on BPM, RR and CRT readings that are perceived as ”normal” or ”abnormal” by medical professionals. However, in reality it is possible that a human could have vital signs outside of the expected boundaries (e.g. a top athlete's HR) and still be perfectly fit and healthy. As this is not common, the synthetic dataset did not have data representing these profiles. The datasets were randomised, split into 5 parts, with 4 parts training, 1 part testing as input into the fuzzy system. The output generated for each of the 5-folds was compared against the expected output and an average of the 5 validation accuracies was calculated, representing the percentage accuracy of the fuzzy logic classifier for synthetic data.

The average 5-fold validation percentage accuracy of the fuzzy logic system for classifying the synthetic datasets was 95.3%. Inaccuracies occurred where there was more than one vital sign in an overlap area of the membership functions. Considering the high performance of the classifier and the understandable reasons for any inaccuracies, the classifier was also tested with the real participant data collected for vital sign measurement in this paper. The participant data were input into the fuzzy system and evaluated in a similar manner to that of the synthetic data.

5.2. Fuzzy Classification Results and Discussion - Real Patient Data

Following validation of the fuzzy logic system using synthetic data in Section 5.1; the data collected from the participants were organised into the same format as the synthetic data, i.e. into datasets containing a calculated BPM, RR and CRT for each set of data collected per participant. The percentage accuracy of the fuzzy logic system for classifying the vital signs calculated from the participants was 72.2%. This is relatively accurate for the determination of a patients health especially considering it is based on three vital signs alone. Furthermore, it is important to note that there were only 36 datasets from human participants in comparison with 90,000 synthetic datasets, meaning each incorrect classification has a greater effect on the overall accuracy percentage. As the data being classified by the fuzzy logic system were the outputs from the BPM, RR in Section 4.1 and

CRT in Section 4.2, then some of the incorrect classifications are cumulative errors. For example, if the BPM, RR or CRT or more than one of them was incorrectly computed then it will not be possible for the fuzzy logic system to correctly classify the participant's health based on incorrect vital sign data. Considering that the accuracies of the algorithms were 97.22%, 91.67% and 88.89% when classifying BPM, RR and CRT respectively, then it is expected that the inaccuracies from these algorithms would cumulate towards inaccuracies during fuzzy logic classification. Therefore, the accuracy presented for real data could potentially be even higher if it cumulatiove errors could be quantified and removed. Furthermore, all 12 participants were healthy and included some very fit participants. Therefore, there were cases where the participants had as low as 6-7 breaths per minute and a BPM of under 60. This meant that at least two of the vital signs were outside what is considered to be normal for an average person. Unfortunately, the system cannot deal with outliers at this time due to lack of previous knowledge about the participant. It is expected that there will be exceptions which mean that some peoples' vital signs lie outside of the expected boundaries even though they are perfectly healthy. In a disaster zone if the system were to encounter any of these exceptions it would merely result in the person being rescued earlier than perhaps needed, which is not a negative outcome. There is no information provided to the system to inform it if the participant is fit and thus it is normal for them to have a lower than average BPM and RR. Furthermore, it is important to reiterate that the assessment of each participant's health is being made from a short, one-off, 60 second monitor for BPM and RR and one measurement of CRT rather than continuous monitoring of their health over a prolonged period of time. Therefore, when the datasets containing such outliers are removed from the fuzzy classification, the accuracy of the fuzzy logic system when classifying the health status of the participants increases to 83.9%. Considering the data for CRT was collected at different times of the day producing different ambient light conditions and from a range of skin colours, the algorithm has proven to be robust. Although the overall accuracy of the fuzzy classification system is lower when classifying participant data than synthetic data, an effective system to classify human health status in an emergency scenario based on a one-off assessment of BPM, RR and CRT has been developed.

6. Conclusion and Future Work

To triage health based on the three vital signs (BPM, RR and CRT), a fuzzy logic classifier was developed. The outputs of the fuzzy logic classifier were developed using the knowledge of a medical professional and by referring to the NHS standard for the assessment of acute illness and severity document (Royal College of Physicians of London, 2012). Although the classifier performed better on informed synthetic data rather than on real data; it still proved to be an effective classifier capable of determining a human's health status from just one assessment of BPM, RR and CRT. This system could be used as part of a robotic triage system in an emergency scenario and play a key role in prioritising victims in an emergency situation.

Methods for detecting, measuring and analysing three human vital signs, namely BPM, RR and CRT were also presented as a pilot study to automatically collect vital signs and inform the fuzzy triage classifier system. The methods presented replicate, to some extent, the methods carried out by medical professionals when measuring these vital signs and could be used to equip a first responder robot. It is clear that accuracies similar to that of a medical professional, can be achieved for the calculation of BPM and RR when using the methods presented in this paper, particularly when using a robust two stage noise reduction algorithm comprising of a low pass filter and a DWT wavelet based smoothing algorithm and a peak/ trough detection algorithm with a semi-automatic thresholding technique. Due to the nature of the data a fully automatic thresholding approach was found to be adequate to gather an estimate of the participant's BPM and RR but not for an accurate calculation, as it was proven to be less accurate. Furthermore, it was found that the addition of a third stage of filtering by means of lateral inhibition did not improve the accuracy of detecting peaks and troughs in the datasets.

It should be noted that when a medical professional is measuring BPM, in the majority of cases they will only measure for 10, 20 or maybe 30 seconds with their fingers on the participant's wrist to ascertain an estimate of their BPM. Although the pulses measured by the medical professional to compare with the accuracy of the system were measured over 60 seconds, there is still a possibility of slight human error. It is clear from the results presented that the artificial system is also capable of such estimates, and indeed accurate measurements of BPM. Often a medical professional is

trying to measure vital signs in an emergency situation and therefore their measurements are not exact and have a slight margin of error as is the case with the algorithms presented. For example, when assessing a person's breathing, a medical professional will simply watch a person's chest for movement when breathing in and out and count how many times this occurs in one minute. In extreme circumstances where vision is inadequate or not possible, the medical professional will rest their hand on the participant's chest and try to determine a breathing rate via touch. The methods presented are capable of such measurements and with similar accuracies.

An algorithm capable of determining a third vital sign of human health, namely CRT was also provided with further details of the algorithm to be found in (Kerr et al., 2018). A human's CRT should normally be less than 2 seconds if they are in a healthy state. The algorithm proved to be effective and robust across a range of skin tones, determining a correct measurement of CRT in 32 of the 36 participant datasets.

The fuzzy triage system in this paper has been trained and validated by a large quantity of informed synthetic data together with a pilot study of real patient data. However, all subjects in the pilot study were human adults. Future work would include expanding this study and data collection to include a wider range of age, gender and race and ultimately form a much greater sized dataset of real human vital signs. This will further validate and optimise the fuzzy triage system as well as further assessing the accuracy of the robotic based methods presented in this paper to measure BPM, RR and CRT. Furthermore, the work in this paper focussed on using the BioTAC fingertip to replicate the role of medical personnels' fingertips when assessing human vital signs. Collecting Electromyography (EMG) data from the arm of medical personnel when conducting standard medical assessments would provide useful knowledge and inform researchers on the correct kinematics for the control of robot arms and hands to conduct similar medical assessments. These methods, coupled with extensive knowledge of materials and objects using methods such as those outlined in (Kerr et al., 2017), could be used to help a robotic system guide a fingertip to the wrist, chest and forehead of a trapped victim and proceed to measure their vital signs. Although some methods have been presented in the literature to identify the health of trapped persons in a disaster or emergency zone, combining tactile sensing with vision to firstly confirm victims in an emergency environment and secondly conduct a medical assessment of them, could prove to be very effective.

References

Ali, A., Shamsuddin, S., Ralescu, A., and Visa, S. (2011). Fuzzy classifier for classification of medical data. In *2011 11th International Conference on Hybrid Intelligent Systems (HIS)*, pages 173–178.

ATi (2017). Ati f/t sensor: Nano17.

Bent, B., Goldstein, B., Kibbe, W., and Dunn, J. (2020). Investigating sources of inaccuracy in wearable optical heart rate sensors. *npj Digital Medicine*, 3:18.

Blaine, R. and Alexandria, D. (2016). Health at hand: A systematic review of smart watch uses for health and wellness. *Journal of Biomedical Informatics*, 63:269–276.

Blej, M. and Azizi, M. (2016). Comparison of mamdani-type and sugeno-type fuzzy inference systems for fuzzy real time scheduling. *International Journal of Applied Engineering Research*, 11(22):11071–11075.

Bohr, A. and Memarzadeh, K. (2020). *The rise of artificial intelligence in healthcare applications*, pages 25–60.

Boothby, A., Das, V., Lopez, J., Tsay, J., Nguyen, T., Banister, R., and Lie, D. (2013). Accurate and continuous non-contact vital signs monitoring using phased array antennas in a clutter-free anechoic chamber. In *2013 35th Annual International Conference of the IEEE Engineering in Medicine and Biology Society (EMBC)*, pages 2862–2865.

Chang, C., Lee, F., Lin, Y., and Yang, Y. (2016). Tunneling piezoresistive tactile sensing array for continuous blood pressure monitoring. In *2016 IEEE 29th International Conference on Micro Electro Mechanical Systems (MEMS)*, pages 169–172.

Choi, J. and Kim, D. (2009). A remote compact sensor for the real-time monitoring of human heartbeat and respiration rate. *IEEE Transactions on Biomedical Circuits and Systems*, 3(3):181–188.

Chong, H. and Gan, K. (2016). Development of automated triage system for emergency medical service. In *2016 International Conference on Advances in Electrical, Electronic and Systems Engineering (ICAEES)*, pages 642–645.

Cios, K. (2001). Fuzzy classifier design. *Neurocomputing*, 36(243):1–4.

Cook, N., Shepherd, A., and Boore, J. (2021). *Essentials of Anatomy and Physiology for Nursing Practice*. SAGE Publications.

Dennis, B. and Muthukrishnan, S. (2014). Agfs: Adaptive genetic fuzzy system for medical data classification. *Applied Soft Computing*, 25:242–252.

Fallow, B., Tarumi, T., and Tanaka, H. (2013). Influence of skin type and wavelength on light wave reflectance. *Journal of clinical monitoring and computing*, 27(3):313–317.

Gault, T. and Farag, A. (2013). A fully automatic method to extract the heart rate from thermal video. In *2013 IEEE Conference on Computer Vision and Pattern Recognition Workshops*, pages 336–341.

Gu, C. and Li, C. (2014). From tumor targeting to speech monitoring: Accurate respiratory monitoring using medical continuous-wave radar sensors. *IEEE Microwave Magazine*, 15(4):66–76.

Hameed, I. (2011). Using gaussian membership functions for improving the reliability and robustness of students' evaluation systems. *Expert Systems with Applications*, 38(6):7135–7142.

Iyer, B., Kumar, A., Pathak, N. P., and Ghosh, D. (2013). Concurrent multiband rf system for search and rescue of human life during natural calamities. In *IEEE MTT-S International Microwave and RF Conference*, pages 1–4.

Jacobson, A. L. (2001). Auto-threshold peak detection in physiological signals. In *Engineering in Medicine and Biology Society, 2001. Proceedings of the 23rd Annual International Conference of the IEEE*, volume 3, pages 2194–2195.

Kerr, E., Coleman, S., McGinnity, T., and Shepherd, A. (2018). Measurement of capillary refill time (crt) in healthy subjects using a robotic hand. In *The IEEE Conference on Computer Vision and Pattern Recognition (CVPR) Workshop, Salt Lake City, USA*, pages 1291–1298.

Kerr, E., Coleman, S., McGinnity, T., and Shepherd, A. (2019). Human pulse and respiratory signal analysis using a robot hand equipped with a biomimetic fingertip. In *International Conference on Artificial Intelligence and Soft Computing (ICAISC), Tokyo, Japan*.

Kerr, E., McGinnity, T., and Coleman, S. (2017). Tactile sensing based material classification. *Elsevier Journal of Expert Systems with Applications*.

Kerr, E., McGinnity, T., Coleman, S., and Shepherd, A. (2015). Towards pulse detection and rhythm analysis using a biomimetic fingertip. In *2015 IEEE International Joint Conference on Neural Networks, July 12-17 2015, Killarney, Ireland*.

King, D., Morton, R., and Bevan, C. (2014). How to use capillary refill time. *Archives of Disease in Childhood - Education and Practice*, 99(3):111–116.

Kuo, H., Lin, C., Yu, C., Lo, P., Lyu, J., Chou, C., and Chuang, H. (2016). A fully integrated 60-ghz cmos direct-conversion doppler radar rf sensor with clutter canceller for single-antenna noncontact human vital-signs detection. *IEEE Transactions on Microwave Theory and Techniques*, 64(4):1018–1028.

Kuo, H. C., Chou, C. C., Lin, C. C., Yu, C. H., Huang, T. H., and Chuang, H. R. (2015). A 60-ghz cmos direct-conversion doppler radar rf sensor with clutter canceller for single-antenna noncontact human vital-signs detection. In *2015 IEEE Radio Frequency Integrated Circuits Symposium (RFIC)*, pages 35–38.

Lai, L., Wittbold, K., Dadabhoy, F., Sato, R., Landman, A., Schwamm, L., He, S., Patel, R., Wei, N., Zuccotti, G., Lennes, I., Medina, D., Sequist, T., Bomba, G., Keschner, Y., and Zhang, H. (2020). Digital triage: Novel strategies for population health management in response to the covid-19 pandemic. *Healthcare*, 8:100493.

Lin, J. (1975). Noninvasive microwave measurement of respiration. *Proceedings of the IEEE*, 63(10):1530–1530.

Lu, G., Yang, F., Jing, X., Yu, X., Zhang, H., Xue, H., and Wang, J. (2011). Contact-free monitoring of human vital signs via a microwave sensor. In *2011 5th International Conference on Bioinformatics and Biomedical Engineering*, pages 1–3.

Luo, J. W., Bai, J., and Shao, J. H. (2006). Application of the wavelet transforms on axial strain calculation in ultrasound elastography. *Progress in Natural Science*, 16(9):942–947.

Mallat, S. G. (1989). A theory for multiresolution signal decomposition: The wavelet representation. *IEEE Trans. Pattern Anal. Mach. Intell.*, 11(7):674–693.

Mamdani, E. (1974). Application of fuzzy algorithms for control of simple dynamic plant. *Electrical Engineers, Proceedings of the Institution of*, 121(12):1585–1588.

Mamdani, E. (1977). Application of fuzzy logic to approximate reasoning using linguistic synthesis. *IEEE Transactions on Computers*, 26(12):1182–1191.

Maritsch, M., Bérubé, C., Kraus, M., Lehmann, V., Züger, T., Feuerriegel, S., Kowatsch, T., and Wortmann, F. (2019). Improving heart rate variability measurements from consumer smartwatches with machine learning. *CoRR*, abs/1907.07496.

MATLAB Fuzzy Logic Toolbox (2013). *MATLAB Fuzzy Logic Toolbox version 8.10.0 (R2013a)*. The MathWorks Inc., Natick, Massachusetts.

Mellado, I. (2013). Uavster website.

Mi, X. and Nakazawa, F. (2014). A multipoint thin film polymer pressure/-force sensor to visualize traditional medicine palpations. In *IEEE SENSORS 2014 Proceedings*, pages 843–846.

Misiti, M., Misiti, Y., Oppenheim, G., and Poggi, J.-M. (2007). *Wavelets and their Applications*. Wiley Publishing.

Murphy, R., Srinivasan, V., Henkel, Z., Suarez, J., Minson, M., Straus, J., Hempstead, S., Valdez, T., and Egawa, S. (2013). Interacting with trapped victims using robots. In *2013 IEEE International Conference on Technologies for Homeland Security (HST)*, pages 32–37.

Naaz, S., Alam, A., and Biswas, R. (2011). Effect of different defuzzification methods in a fuzzy based load balancing application. *IJCSI-International Journal of Computer Science Issues*, 8(5).

Nguyen, T., Khosravi, A., Creighton, D., and Nahavandi, S. (2015). Medical data classification using interval type-2 fuzzy logic system and wavelets. *Applied Soft Computing*, 30:812–822.

Obo, T., Sawayama, T., Sawayama, T., and Kubota, N. (2017). Vital sign detection system during bathing using ultrasensitive vibration sensor. *Transactions of the Institute of Systems, Control and Information Engineers*, 30(7):263–272.

Pal, S. and Mandal, D. (1991). Fuzzy logic and approximate reasoning: An overview. *IETE Journal of Research*, 37(5-6):548–560.

Qian, Y., Song, A., and Yan, R. (2011). Design and realization of an array pulse detecting tactile sensor. In *2011 IEEE International Instrumentation and Measurement Technology Conference*, pages 1–5.

Ramos-Garcia, R., Da Silva, F., Kondi, Y., Sazonov, E., and Dunne, L. (2016). Analysis of a coverstitched stretch sensor for monitoring of breathing. In *2016 10th International Conference on Sensing Technology (ICST)*, pages 1–6.

Reichardt, W. and MacGinitie, G. (1962). Zur theorie der lateralen inhibition. *Kybernetik*, 1:155–165.

Ren, L., Wang, H., Naishadham, K., Liu, Q., and Fathy, A. (2015). Noninvasive detection of cardiac and respiratory rates from stepped frequency continuous wave radar measurements using the state space method. In *2015 IEEE MTT-S International Microwave Symposium*, pages 1–4.

Rolfe, S. (2019). The importance of respiratory rate monitoring. *British Journal of Nursing*, 28(8):504–508.

Royal College of Physicians of London (2012). *National Early Warning Score (NEWS): Standardising the Assessment of Acute-Illness Severity in the NHS*. Royal College of Physicians of London.

Samani, H. and Zhu, R. (2016). Robotic automated external defibrillator ambulance for emergency medical service in smart cities. *IEEE Access*, 4:268–283.

Šprager, S., Donlagić, D., and Zazula, D. (2012). Overnight heartbeat monitoring by using unobtrusive optical interferometric measurements. In *2012 IEEE-EMBS Conference on Biomedical Engineering and Sciences*, pages 847–852.

Syntouch (2013). The syntouch website.

Tam, H., Chung, S., and Lou, C. (2018). A review of triage accuracy and future direction. *BMC Emergency Medicine*, 18.

Tasli, H., Gudi, A., and den Uyl, M. (2014). Remote ppg based vital sign measurement using adaptive facial regions. In *2014 IEEE International Conference on Image Processing (ICIP)*, pages 1410–1414.

Tedesco, S., Sica, M., Sica, A., Timmons, S., Barton, J., and O'Flynn, B. (2019). Accuracy of consumer-level and research-grade activity trackers in ambulatory settings in older adults. *PloS one*, 14(5):e0216891–e0216891.

Tran, D., Lee, H., and Kim, C. (2015). A robust real time system for remote heart rate measurement via camera. In *2015 IEEE International Conference on Multimedia and Expo (ICME)*, pages 1–6.

UK, R. C. (2021). The abcde approach.

Walraven, G. (2011). *Basic Arrhythmias*. EKG Series. Pearson.

Weiler, D., Villajuan, S., Edkins, L., Edkins, C., Edkins, S., and Saleem, J. (2017). Wearable heart rate monitor technology accuracy in research: a comparative study between ppg and ecg technology. In *Proceedings of the Human Factors and Ergonomics Society Annual Meeting*, volume 61, pages 1292–1296. SAGE Publications Sage CA: Los Angeles, CA.

Wu, H.-Y., Rubinstein, M., Shih, E., Guttag, J., Durand, F., and Freeman, W. (2012). Eulerian video magnification for revealing subtle changes in the world. *ACM Trans. Graph. (Proceedings SIGGRAPH 2012)*, 31(4).

Zadeh, L. (1965). Fuzzy sets. *Information and Control*, 8(3):338–353.

Zimmermann, H. (2001). *Fuzzy Set Theory - and Its Applications*. Springer Netherlands.